Laminar Natural Convection Heat Transfer to Air from a Vertically Arranged Array of Horizontal Cylinders

Yasin K. Salman
Professor
Energy Engineering Department
College of Engineering
University of Baghdad

Humam Salih Mahdi
Energy Engineering Department
College of Engineering
University of Baghdad

ABSTRACT
Natural convection heat transfer to air from a bank of four horizontal aluminum cylinders vertically lined and subjected to an identical constant heat flux has been examined experimentally. Each cylinder in the bank has 30 mm outer diameter, 2 mm thickness and 400 mm in length. The investigation covered five cylinders center to center spacing (2D, 2.5D, 3D, 4D, and 5D) and five identical cylinder heat fluxes which varied the modified Rayleigh number (Ra_D^*) from $6{,}1x10^5$ to $2.0x10^6$. The outcomes demonstrate that the local Nusselt number increases as the heat flux and cylinders center to center spacing increasing. The heat transfer results for the second, third and fourth cylinders are more down than the first cylinder heat transfer solution. The differences of the three cylinders in comparison with first cylinder are improving gradually as the cylinder center to center spacing increasing and that can be attributed to the natural convection current interaction. The temperature profile around the cylinder circumference indicates that the maximum Nusselt number occurs at $\theta = 0^o$ (cylinder bottom leading edge) and the maximum surface temperature and lower Nusselt number occurs at $\theta = 180^o$ (top of the cylinder).. Empirical correlations were obtained for the average Nusselt number as a function of the modified Rayleigh number. Empirical formulas by which heat transfer characteristic form each individual cylinder in the array evaluated and listed in comparison with first cylinder showing the effect of cylinder center to center spacing.

Keywords
Natural Convection, horizontal cylinders array vertically line up, cylinder center to center spacing.

1. INTRODUCTION
Heat is defined as an energy that flow between systems or system and its surrounding due to difference in temperature. Heat flows in a direction from higher to lower temperature. This energy can neither be measured nor be observed directly. Free convective heat transfer has always been of particular interest among heat transfer problems. In free convection process, fluid motion is caused by density variations resulting from temperature. In the last three decades an interesting results have been presented. The free convection from cylinders or tubes of circular shapes have been receiving growing interest in the last few decades because of its employment in many practical fields in the area of energy conservation, design of solar collectors, heat exchangers, nuclear engineering, cooling of electrical and electronic and many others[1]. Hannani et-al [2], (2001), studied Laminar natural convection from an array of horizontal isothermal cylinders confined between two vertical parallel walls, at low Rayleigh numbers, is investigated by theoretical and numerical methods. The top of the walls is kept constant, however, a figure of the cylinders and their spacing, the space between the walls and Rayleigh number have been deviated. The optimal spacing (confining walls) and the maximum Nusselt number predicted theoretically are validated by means of numerical simulations. The outcomes of this survey reveal that there lives a distance between the confining walls for which the Nusselt number is maximized. By increasing the number of cylinders or their spacing, or, decreasing the Rayleigh number the optimal spacing will increase. Moreover, by increasing Rayleigh numbers, cylinder to cylinder spacing and number of cylinders (if their spacing "S" is large), Nu will increase more than 40%. Haldar et-al [3] (2007), Studied Conjugated numerical solution of laminar free-convection about a horizontal cylinder with external longitudinal fins of finite thickness has been borne away. Fibs alone contributed very little to the total heat transport, but they greatly determine the heat transport from the uncovered area of the cylinder. Among the various fin parameters, thickness has the greatest influence on heat transfer. The rate of heat transfer is above that of the three cylinder only when the attached fins are very thin. For thin fins, there exists a fin length, which maximizes the charge per unit of heat transfer. The optimal number and dimensions length of the fins were obtained as 6 and 0.2 respectively when fin thickness is 0.01. The effect of films on heat transport from the cylinder was found negative except for very thin fins. For thin fins, there exists a fin length, dependent of the number of fins, at which the rate of heat transfer is maximized. The thermal conductivity of fins was found to have little effect on heat transfer. Flori1 and Vîlceanu1 [4], (2014), considered a computational fluid dynamic (CFD) numerical simulation is used to place the fluid flow and heat transfer in the air surrounding a heated horizontal cylinder. The example is created in 2D space dimension involving a finite element solver of Navier-Stokes equations. As natural convection phenomenon is induced by a variable fluid density field with temperature rising, a finite element analysis of free convection around a heated horizontal surface was done to determine the temperature and velocity distributions in the air surrounding environment. Besides initial and boundary conditions, the influence of gravity on air stream rounds the cylinder was expressed in terms of volume force, estimation was used to represent the variable density filed with temperature going up. Hanlari et-al [5] (2015), investigated numerically natural convection heat transfer on aligning arrangement tube banks by using the computational fluid dynamics to change the rate Nusselt number of fluids around the pipes. The fluid was considered to be Newtonian, laminar and steady -state with Boussinesq approximation. The tube diameter is used 30 cm, the number of tubes is six to eight and the temperature air is 300 K, the ratio of longitude distance of cylinder diameter and the ratio of transverse

distance of cylinder diameter was changed in the range of 1.5, 2 and 3. It has noted that the changing in longitudinal and transverse distances between tubes in tube banks has not conduced to a regular process to increase or lessen the average Nusselt number. The Rayleigh number is changed from 106 to 108 from the results the maximum heat transfer rate was in the case with debt/D=2, DL/D=2 and Ra= 108. Al-Mahroom [6], (2000), experimentally investigated the natural convection heat transfer from a horizontal circular cylinder placed in a vented square enclosure with symmetrical openings on the bottom and the upper side of the enclosure. The study included temperature measurements to obtain the Nusselt number and flow visualization to display the current figures. The following Nusselt number formula was correlated for unbounded horizontal cylinder for experimental validation and comparisons: Nu = 0.6 Ra0.212. Olivier Reymond et al. [7], (2008), experimentally investigated the natural convection heat transfer from a single horizontal cylinder and a pair of vertically aligned horizontal cylinders, presents heat transfer distributions around the circumference of the cylinders for Rayleigh numbers of 2×106, 4×106 and 6×106 and a range of
.

2. EXPERIMENTAL APPARATUS AND PROCEDURE

2.1 Description of Apparatus

A schematic diagram and photograph of the device assembly of the apparatus are presented in Figure 1. The apparatus comprises essentially of four aluminum heated cylinders (L) with 30 mm external diameter, 2mm cylinder wall thickness, and 400 mm long (L/D = 13.33). Each heated cylinder fitted with cylindrical Teflon pieces (A) and (B) one on each cylinder end. Each piece, of 120 mm long Teflon rod machined with 30 mm outside diameter (same as cylinder outer diameter) and at one end the diameter was reduced to 26 mm for 20mm long to allow this end to be inserted inside the cylinder. The cylinder components (Teflon piece A + cylinder L + Teflon piece B), which has a total length of 600 mm are held horizontally by the carbon steel structure (S). Teflon was chosen for good machinability behavior and an isolation material as its low thermal conductivity in order to reduce the heat loss from the cylinder ends.

The four cylinders bank is held by a well selected frame of the two carbon steel structure. The cross-section of this carbon steel structure (S) with the help of eight threaded U shape bolts and nuts (H) makes this structure provides a way to hold the four heated cylinders horizontally and to adjust the cylinders center to center spacing variable. The base of the carbon steel structure with four cylinders is mounted on adjustable drawing table (W). Adjusting the table inclination angle about its horizontal spindle can vary the bank inclination angle related to bank vertical situation.

In figure 1, the photograph also shows all the measuring equipment, thermocouples distribution along the outer surface of the bank cylinders and the Teflon piece.

The inner surface of each cylinder in the bank is electrically heated by means of nickel – chromium wire (heating element (D) of 0.3 mm in diameter, wounded in 6 mm diameter helical shape, 400 mm long and with 93Ω total resistance. The helical wire is surrounded 9 mm Pyrex thermal glass tube (E) and located centrally in the aluminum cylinder by the help of the two Teflon pieces. Two ceramic heater ends pieces (N) of 12 mm in diameter and 12 mm long holding the Pyrex thermal glass and through which the heater electrical terminals pass and by which the heater connected to the heater electrical circuit. The ceramic pieces are resting in the Teflon pieces in such a way making the heater helical portion cover all the cylinder (L) length. The space between the Pyrex thermal glass and the cylinder inner surface has been filed completely with manganese oxide powder (M) in order to prevent air trapped inside the cylinder and to create a uniform heat flux during heating.

The cylinder outside temperature distribution is measured axially by eight thermocouples and circumferentially by four thermocouples. The position of these thermocouples a long and around the heated cylinder, which is identical for the four heated cylinders. After the location of all thermocouples marked on the cylinders outer surfaces, a 1.6 mm in diameter holes drilled through the cylinders surface then a 2 mm drill and 1 mm deep was used to chamfer all Thermocouples holes. Thermocouples measuring junctions were inserted inside cylinder from both ends of the cylinder and fixed firmly using Defcon adhesive to the cylinder surface. All excess adhesive was removed during cleaning up the cylinders outer surfaces. Two thermocouples are fixed in the cylindrical Teflon piece (A) shell with 10 mm to estimates the conduction heat transfer loses from the heated cylinder. A thermocouple is located far from the heated cylinders to measure the ambient temperature. All thermocouples terminals left from both device sides and approximately 150 mm far from the carbon steel structure a copper lead wires are used complete the thermocouples circuit. The measuring head of all thermocouples were made by fusion the ends of the thermocouples two wires together by Appling an electric spark.

2.2 Experimental Procedure

The experimental works was accomplished during approximately a continuous three months (from January. 2015 to the end of March 2016) including the verification and repeating some of the suspicious test runs. Natural convection test required very long time to accomplish the steady state condition in comparison with forced convection. For the experimental work period, the time consumed between 10-12 working hours per day.

The procedure followed for each test run is listed as below:

1. The test apparatus prepared to ensure the full functioning of all constituents.
2. The required inclined angle was set by rotating the drawing table about the horizontal spindle to assure that the bank vertical.
3. The supply power to the electric heaters was switched on, and it was adjusted by variac to obtain the required constant heat flux, see figure 1. The value of the voltage and current was indicated by the digital voltmeter and ammeter.
4. Tubes heaters switched on and the voltage and current been recorded.
5. Thermocouples readings monitored by the data logger for each 15 minutes. As the variac is not stabilized so the voltage required also to monitored and adjusted to be constant during the test period.
6. The above procedure took (9-10) hours to achieve the steady state case. Then the following reading was recorded:

a-The cylinders center to center spacing (as the four cylinders center to center spacing cases are 2D, 2.5D, 3D ,4D and 5D, respectively).

b- The power supply to the heating elements presented by the element current and voltage.

c. All thermocouples reading includes the 44 thermocouples along and around the four heated cylinders, the two thermocouples inserted in the Teflon piece and the thermocouple for the ambient temperature.

2.3 Experimental Data analysis

The outcome of the experimental apparatus described in this chapter is to provide an experimental data from which can demonstrate the heat transfer process behavior of each individual cylinder in the bank. The cylinder surface was subjected to a uniform and constant heat flux situation. The experimental data analyzed following the calculation sequences represented below. The total power (Q_T) supplied to the cylinder was calculated as follows:

$$Q_T = V \times I \quad (1)$$

The rate of convection and radiation heat transferred (Qcr) from the cylinder surface is obtained after subtraction the rate of conduction heat loss (Qcond) through the two Teflon pieces from the total input power:

$$Q_{cr} = Q_T - Q_{cond} \quad (2)$$

Where the axial conduction heat loss (Q_{cond}) which was found experimentally equal to approximately 3% of the total input power after using one dimensional steady state Fourier equation :

$$Q_{cond} = -K_{Tef} . A_{Tef} . (\Delta T_{Tef} / \Delta X_{Tef}) \quad (3)$$

Where K_{Tef} is the thermal conductivity for the Teflon material. While A_{Tef} is the Teflon piece annular cross-sectional areas and ΔT_{Tef} and ΔX_{Tef} represent the temperature difference and axial distance between the two thermocouple inserted in the Teflon piece respectively. The convection and radiation heat flux (q_{cr}) can be represented by:

$$q_{cr} = (Q_{cr})/As \quad (4)$$

Where ($A_S = \pi DL$) account for the aluminum cylinder surface area

The convection heat flux which is applied to estimate the local heat transfer coefficient is obtained after deducing the radiation heat flux (q_r) from (q_{cr}) value. Due to low temperature difference between any cylinders in the bank with the other cylinders so the radiation exchange between these cylinders. Therefore, the shape factor between these cylinders is ignored and The local radiation heat flux between each cylinder and the surrounding at ambient temperature can be computed as follows after assuming shape factor equal F = 1 :

$$q_r = F \sigma \varepsilon ((t_s + 273)^4 - (\overline{t_a} + 273)^4) \quad (5)$$

Where σ is Stefan-Boltzmann constant =5.67×10^{-8} W/K^4 and ε represents the emissivity of the polished aluminum surface. Hence the convection heat flux at any position is:

$$q_c = q_{cr} - q_r \quad (6)$$

The local heat transfer coefficient can be obtained as:

$$h_x = \frac{q_c}{(T_s)_x - (T_a)} \quad (7)$$

where: (T_a) is the ambient temperature.

All the air properties were evaluated at the mean film air temperature:

$$(T_f)_x = \frac{(T_s)_x + (T_a)}{2} \quad (8)$$

Where :$(T_f)_x$ is the local mean air film temperature at X.

The local Nusselt number for the cylinder Nu_x then can be determining as:

$$Nu_x = \frac{(h_x)D}{k} \quad (9)$$

$$\overline{T_s} = \frac{1}{L} \int_{x=0}^{x=L} (T_s)_x \, dx \quad (10)$$

$$\overline{T_f} = \frac{\overline{T_s} + Ta}{2} \quad (11)$$

The mean heat transfer coefficient and the beverage Nusselt number (Nu_m) based on the computation of the average tube surface temperature and the average bulk air temperature were calculated as follows:

$$\overline{h} = \frac{1}{L} \int_{x=0}^{x=L} h_x \, dx \quad (12)$$

$$Nu_m = \frac{q \; D}{k(\overline{T_s} - Ta)} \quad (13)$$

$$Gr_m = \frac{g \; \beta \; D^3 (\overline{T_s} - Ta)}{v^2} \quad (14)$$

Where $\beta = \frac{1}{(273 + \overline{T_f})}$

The modified Grashof (Gr_D*) which based on the surface heat flux is calculated as:

$$Gr_D^* = \frac{g \; \beta \; D^4 \; q_c}{v^2 \; k} \quad (15)$$

$$Pr = \frac{\mu C_p}{k} \quad (16)$$

$$Ra_D = Gr_D . Pr \quad (17)$$

$$Ra_D^* = Gr_D^* . Pr \quad (18)$$

All the air physical properties ρ, μ, v and k were evaluated at the average mean film temperature ($\overline{T_f}$) Holman (2010) [8].

A computer program in FORTRAN was written with algorithm capable to manipulate the data set calculation of air all properties locally and doing and select best equations which fit surface temperatures and local heat transfer coefficients and then doing the numerical integration to obtain the average value for heat transfer coefficient and dimensionless groups for the whole cylinder.

2.4 Experimental Uncertainty

Generally the accuracy of experimental results depends upon the accuracy of the individual measuring instruments and the manufacturing accuracy of the circular tube. The accuracy of an instrument is also limited by its minimum division (its sensitivity). In the present work, the uncertainties in heat transfer coefficient (Nusselt number) and Rayleigh number were estimated following Kline and McClintock differential approximation method reported by Holman [9]. For a typical experiment, the total uncertainty in measuring the heater input power, temperature difference (Ts-Ta), the heat transfer rate and the circular tube surface area were 0.38%, 0.48%, 2.6%, and1.3% respectively. These were combined to give a maximum error of 2.12% in heat transfer coefficient (Nusselt number) and maximum error of 2.51% in Rayleigh number.

3. RESULTS AND DISCUSSION

The variation of the temperature along the cylinder axial position for the second cylinder in the bank and for five surface fluxes is demonstrated in figure 2 while the temperature distribution for the fourth cylinder is shown in figure 3. The first cylinder (lower cylinder) in the bank always unaffected with other cylinders in the bank as expected, but first cylinder natural convection flow can affect the second cylinder heat transfer. From these two figures, and for the same surface heat flux, the temperature distribution for the fourth cylinder is approximately lower than the second cylinder and that can be attributed to second and third cylinders buoyant flow interaction with the fourth cylinder flow which can change the laminar boundary layer to turbulent boundary layer and augment the heat transfer process.

The effect of changing the cylinders center to center spacing on the temperature distribution along the cylinder for the horizontal cylinders in vertically arranged bank presented in figures 4 and 5. The temperature distribution demonstrated for the hight heat flux (1141.64 W/ m^2) and for second and fourth cylinders in figure 4 and figure 5, respectively. In figure 3, for second cylinder, all the temperature distribution have the same general distribution but the figure clearly shows that the 2D center to center spacing recorded the highest temperature distribution and on average temperature values decreases with increasing the cylinder center to center spacing (S The natural convection current interference in 2D spacing was still higher the others cylinder spacing so that creates an average surface temperature for 2D spacing highest values in comparison with other spacing. The temperature distribution for the fourth cylinder and for high heat flux which depicted in figure 5 has similar general shape shown in figure 4 but the real reduction in average surface temperature beyond 2D cylinder center to center spacing. This behavior reveals that natural convection currents interference depends on the cylinders center to center spacing and the subjected cylinders heat flux. The stability of natural convection plumes in external flow conditions demonstrated in literature is very difficult to achieved experimentally and that makes the accomplished of steady state required a very long time.

Figure 6 has been selected to show the temperature distribution along the four cylinders for 2D spacing and for high heat flux (1141 W/m^2). In this figure, the temperature distribution for second cylinder is the highest and the temperature distribution decreases with cylinder three but still higher than first cylinder while the distribution along fourth cylinder decreases further to becomes even lower than first cylinder number one in the bank. Therefore, the cylinder average surface temperature for second cylinder is the highest temperature recorded in the bank while third and fourth cylinders recorded temperature around the first cylinder. Results show that the fourth cylinder has the best heat dissipation in the bank. This can be attributed interference of the natural convection currents from the lower cylinder to create a situation of mixed convection or change the flow mode from laminar to turbulent flow on the fourth cylinder. The temperature distribution along four cylinders and for the cylinder center to center 5D presented in figures 7 and high heat flux (1141.64 W/m^2). In this figure, the temperature distribution along the cylinders axis is approximately collapse on a single horizontal line. Results indicate the diminishing of natural convection current interference as the results of the second, third and fourth cylinders in the bank have a similar distribution obtained for the first cylinder.

The effect of the heat flux subjected to the cylinder surface on the local heat transfer coefficient, which represented by the local Nusselt number $Nu_{D,x}$ is depicted along the cylinder, for the second cylinder in figure 8 . For the specific heat flux subjected to the surface, the figure shows almost a constant local Nusselt number along whole the cylinder with a slight variation in the local Nusselt number $Nu_{D,x}$ at the cylinder both ends. This variation if exist can be attributed to the conduction heat loss. The behavior shown in figure 8 repeats for other cylinders in the bank in which the local Nusselt number $Nu_{D,x}$ increases with the increasing cylinder heat flux. This trend is expected as the heat flux increasing the surface temperature increasing accordingly and that improves the buoyancy driven forces on the cylinder outer surface increasing the buoyancy current velocity and that improving heat transfer process.

The effect changing the cylinders center to center spacing (S) on the cylinders local heat transfer coefficient along the bank cylinders is presented in figure 9. Variation of local Nusselt Number $Nu_{D,x}$ along the cylinder axial dimensionless distance (X/D), for the second cylinder in the bank , and for high heat flux (1141.64 W/m^2) is shown in figure 9 . This figure revels that heat transfer increased with the increasing cylinders center to center spacing and also reveals that the cylinder heat transfer increases with the increasing cylinder heat flux. The improvement in the heat transfer coefficients created mainly by the cylinders currents interference. The comparison of the second and fourth cylinders results reveal that the local Nusselt number $Nu_{D,x}$ range variation for all cylinders center to center spacing and for fourth cylinder is higher than for second cylinder and for both low and high heat fluxes. That indicates that the fourth cylinder in the bank has a better heat transfer dissipation. The variation of the local Nusselt number $Nu_{D,x}$ with dimensionless axial distance (X/D), for four cylinders in the bank and for cylinders center to center spacing (2D) is presented for high heat flux in figure 10. For the high flux the third and fourth cylinders results give a higher heat transfer coefficient in comparison with first cylinder in the bank while the second cylinder results give lower heat transfer coefficient in comparison with first cylinder.

The experimental results were correlated for the first cylinder in the bank which was expected to be unaffected by the other bank cylinders and to be used as a control cylinder. The correlation for 25 runs is presented in the following empirical equation:

$$Nu_{D,L} = 0.48Ra_D^{0.232} \qquad (19)$$

The above equation was presented in figure 11 which shows the variation of average Nusselt number ($Nu_{D,L}$) with the modified Grashof number (Ra_D) in a logarithmic scale.. This equation is in a good agreement with the available empirical equation presented in the previous available works Raymond et-al [7](2008) , figure 12 shows a variation of bank cylinders average Nusselt Number versus average Rayleigh number for cylinder center to center spacing (2D) and with reference to cylinder no.1. Table 1 summarized the correlation equation for the other cylinders in the bank presented in equations for the average Nusselt number ($Nu_{D,L}$) with the modified Grashof number (Ra_D). These equation in this table presented for five cylinders spacing (s) (2D, 2.5D, 3D, 4D, and 5D). The table also shows the percentage deviation of the three cylinders second, third and fourth cylinders results from the control first cylinder result and for the range of modified Grashof number examined.

4. CONCLUSIONS

1- The heat transfer process improves by increasing the heat flux and cylinders center to center spacing to become even better than the heat transfer from a single horizontal cylinder.

2- The average cylinders surface temperature values decrease with increasing the cylinder center to center spacing (S) for the same heat flux subjected to the cylinder bank.

3- For all the bank cylinders and for all cylinders center to center spacing, the local Nusselt number increases with increasing the value of the applied cylinder heat flux.

4- The fourth cylinder (in the top position) and for the cylinder's center to center spacing other than (5D), throws the best heat transfer dissipation in comparison with other bank

Cylinders due to the consequence of lower cylinders natural convection plumes which may be change the flow on this cylinder from laminar to turbulent or created a sort of mixed convection heat transfer regime on it as depicted.

5- when the cylinder center to center spacing is (5D) the natural convection currents for all cylinders have no intervention so the second, third and fourth cylinders in the bank have a similar temperature distribution which obtained for the first cylinder .

6- Average data correlations for the bank cylinders presented and for the range of modified Rayliegh number tested between 5.0x105to 2x106.

5. ACKNOWLEDGMENTS

The author gratefully acknowledges the financial support for this study received from the Energy Department, College of Engineering, University of Baghdad.

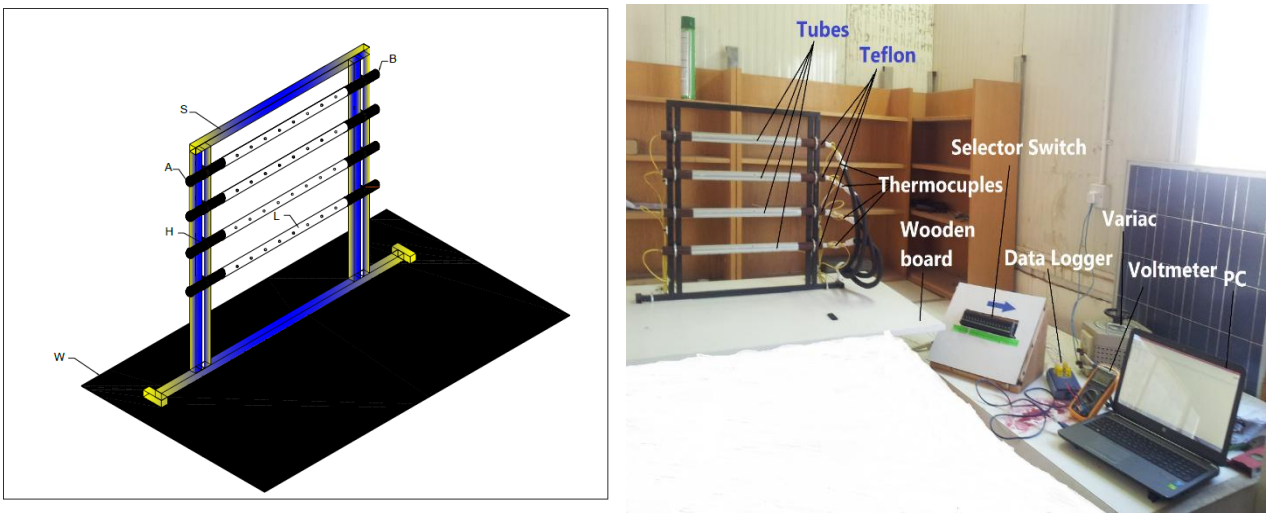

Fig 1: apparatus assembly and photograph for the apparatus and measuring devices

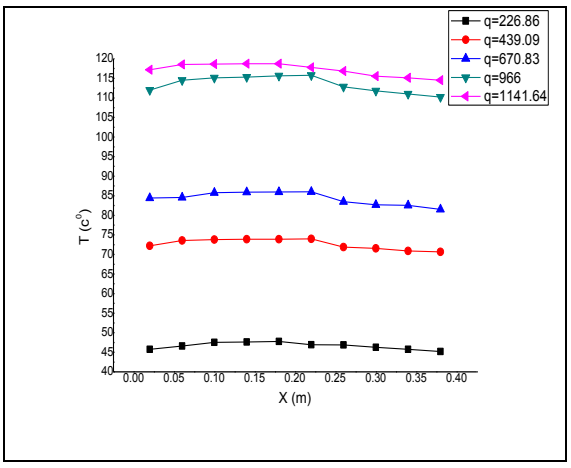

Fig 2: Variation of surface temperature for second cylinder with the cylinder axial distance for different heat fluxes.

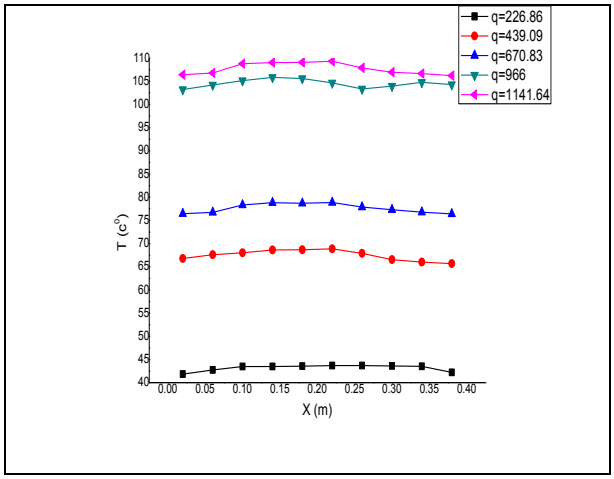

Fig 3: Variation of fourth cylinder surface temperature with the cylinder axial distance for different heat fluxes.

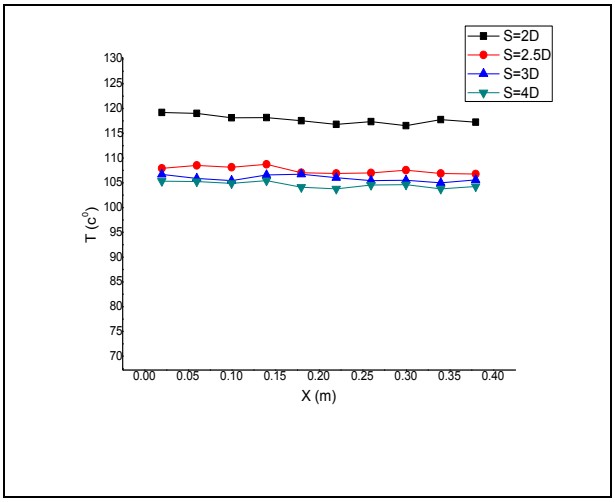

Fig 4: Second cylinder surface temperature variation with the cylinder axial distance for different cylinders spacing (s) and for. q=1141.64 W/m^2.

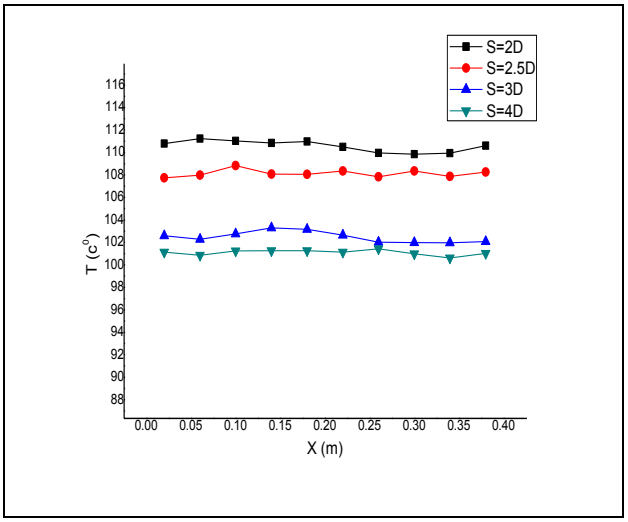

Fig 5: Fourth cylinder surface temperature variation with the cylinder axial distance for different cylinders center to center spacing and for q=1141.64 W/m^2

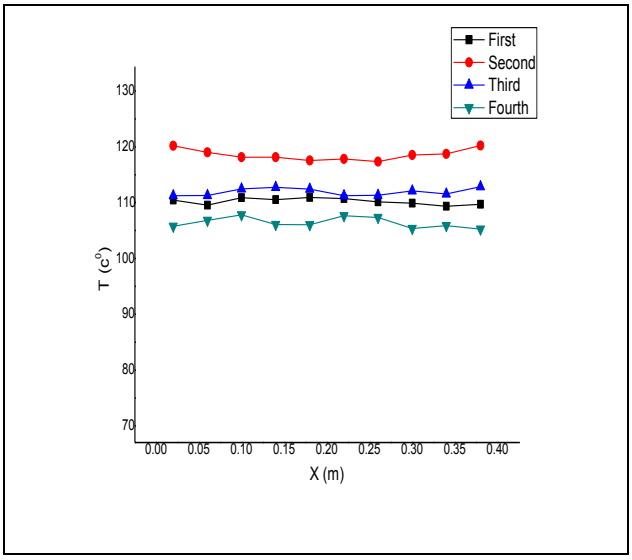

Fig 6: Variation of bank cylinders surface temperature with the cylinder axial distance for cylinders spacing (s) (2D) and for q= 1141.64 W/m^2

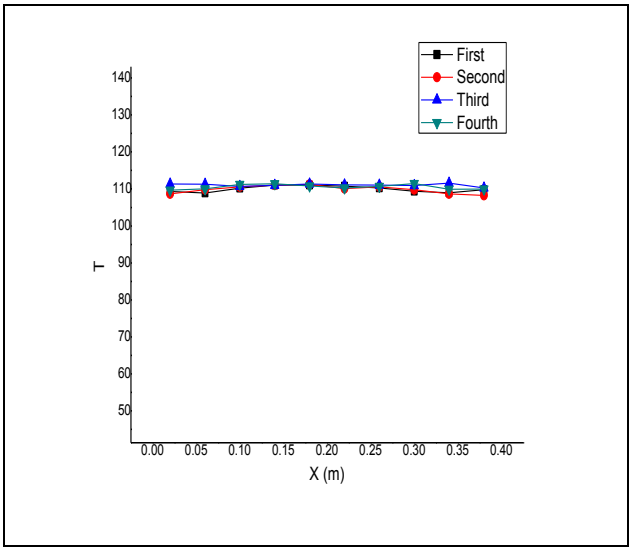

Fig 7: Cylinders surface temperature variation with the axial distance for cylinders spacing (5D) and for q= 1141.64 W/m^2.

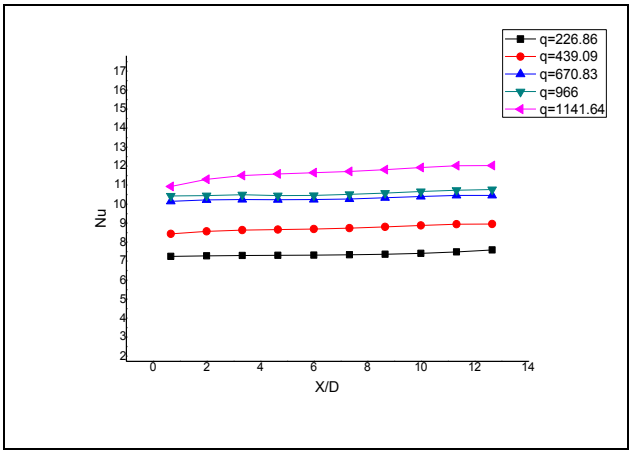

Fig 8: Variation of second cylinder local Nusselt number with dimensionless axial distance(X/D) for different heat fluxes.

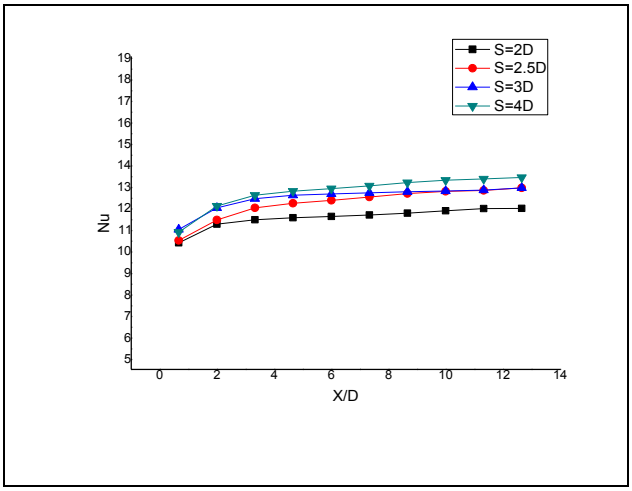

Fig 9: Variation of second cylinder local Nusselt number with dimensionless axial distance(X/D) for different cylinders spacing and for q=1141.64 W/m^2.

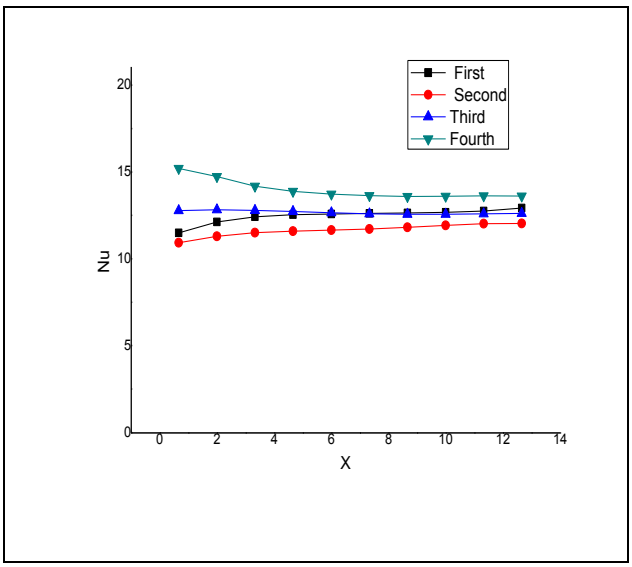

Fig 10: Variation of bank cylinders local Nusselt number with the dimensionless axial distance(X/D) for cylinders center to center spacing (2D) for q=1141.64W/m^2.

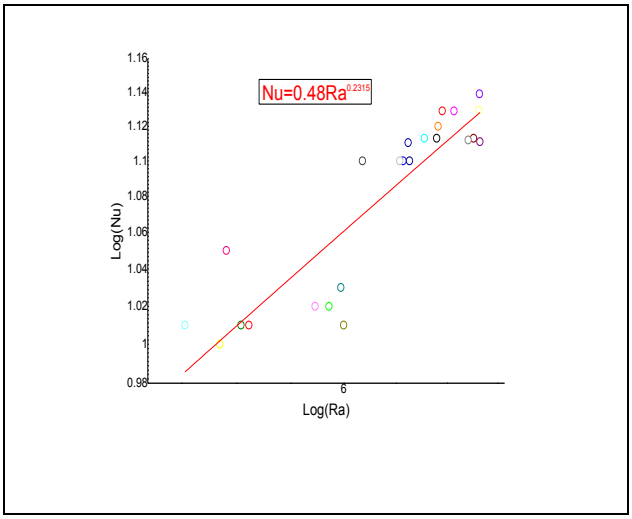

Fig 11: Average Nusselt Number versus average Rayleigh number For the First cylinder in the bank.

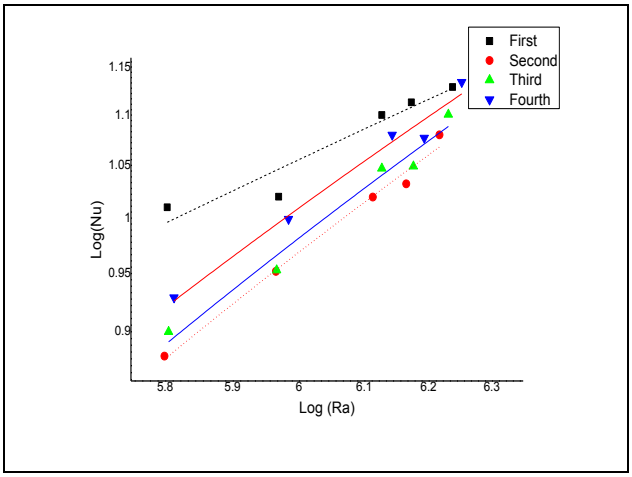

Fig 12: Variation of bank cylinders average Nusselt Number versus average Rayleigh number for cylinder center to center spacing (2D).

Nomenclature

A_S Tube surface areas (m^2)

Cp Specific heat at constant pressure, (kJ/kg.K)

D Tube diameter (m)

F_{1-2} view factor between tube and walls

Gr_m Mean Grashof number, ($g\beta\ qD^4/k\ 2$

g Gravitational acceleration (m/s^2)

h_X Local heat transfer coefficient ($W/m^2.K$)

h_m Average heat transfer coefficient ($W/m^2.K$)

I Heater current, (Amp.)

K Thermal conductivity (W/m.K)

L Axial length of the tube (m)

Nu_X Local Nusselt number, $h_X.D/K$

Nu_m Mean Nusselt number

Pr Prandtl number, ($\mu.C_p/k$)

Q_C Heat transfer by convection, (W)

Q_{Cond} Heat transfer by conduction (W)

Q_T Total heat input (W)

Q_{cr} Heat transfer by convection and radiation (W)

qc Convection heat flux (W/m2)

qr Radiation heat flux (W/m2)

qcr Convection – radiation heat flux (W/m2)

R Tube radius (m)

Ra_m Mean Rayleigh number, $G_m.Pr$

$(T_s)_x$ Local tube surface temperatures (C^o)

T_S Average tube surface temperature (C^o)

V Heater voltage, (volt)

X* Dimensionless axial distance, X/D

Greek symbols

β Coefficient for volumetric thermal expansion (K^{-1})

ε Emissivity; inner surface and outer surface

μ Fluid viscosity (kg/m.s)

ν Kinematics viscosity (m^2/s)

ρ Fluid density (kg/m^3)

σ Stefan-Boltzmann constant ($W/m^2.K^4$)

6. REFERENCES

[1] Dennis J. Wessel, George Reeves, "Ashrae Hand Book fundamentals" (2001).

[2] S. Kazemzadeh Hannani, M. S. Sadeghipour and M. Nazaktabar "Natural convection heat transfer from horizontal cylinders in a vertical array confined between parallel walls" IJE Transactions A: Basics, Vol. 15, No. 3, September (2001).

[3] S.C. Haldar, G.S. Kochhar and K. Manohar. "Numerical Study of Laminar Free Convection about a Horizontal Cylinder with Longitudinal Fins of Finite Thickness" International Journal of Thermal Sciences, (2007).

[4] M Flori and L Vîlceanu. "CFD numerical simulation of air natural convection over a heated cylindrical surface" International Conference on Applied Sciences (2014).

[5] Soroush Mirzak hanlari; Behnam pourJalal, Aran Alaie sheikhrobat, Temour Behzadi. "Numerical investigation of Natural convection heat transfer on aligned arrangement tube banks" International conference on

[6] Al-Mahroom F. G. F. (2000), "Natural Convection Heat Transfer from a Horizontal Cylinder Placed In a.

[7] O. Reymond, D. B. Murray and S. O'Donovan, (2008) "Natural Convection Heat Transfer from Two Horizontal Cylinders" Experimental Thermal and Fluid Science, vol. 32, pp: 1702-1709, June.

[8] Holman J. P. (2010). "Heat transfer", 10th edition, McGraw-Hill Series in Mechanical Engineering,

[9] Jack P. Holman. (2011). "Experimental methods for engineers", 8th ed. McGraw-Hill Series in Mechanical Engineering

Table 1: The empirical formulas for the second, third and fourth cylinders in the bank and the percentage deviation from the first cylinder in the bank:

Cylinder number in bank	Empirical equation	% deviation from equation (17) at low Ra_D^*	% deviation from equation (17) at high Ra_D^*	Cylinders center to center spacing
second	$Nu_{D,L} = 0.01708\ Ra_{D,L}^{0.456}$	-28.6	-9.8	2D
third	$Nu_{D,L} = 0.016202\ Ra_{D,L}^{0.462}$	-26.7	-6.9	2D
fourth	$Nu_{D,L} = 0.02166\ Ra_{D,L}^{0.446}$	-21.24	-1.64	2D
second	$Nu_{D,L} = 0.03214\ Ra_{D,L}^{0.415}$	-22.14	-5.6	2.5D
third	$Nu_{D,L} = 0.03849\ Ra_{D,L}^{0.405}$	-19.02	-3.05	2.5D
fourth	$Nu_{D,L} = 0.03175\ Ra_{D,L}^{0.419}$	-19.02	-1.04	2.5D
second	$Nu_{D,L} = 0.0974\ Ra_{D,L}^{0.339}$	-14.85	-5.1	3D
third	$Nu_{D,L} = 0.0558\ Ra_{D,L}^{0.379}$	-16.37	-2.5	3D
fourth	$Nu_{D,L} = 0.0887\ Ra_{D,L}^{0.347}$	-13.5	-3.5	3D
second	$Nu_{D,L} = 0.0292\ Ra_{D,L}^{0.435}$	-10.54	5.8	4D
third	$Nu_{D,L} = 0.0298\ Ra_{D,L}^{0.427}$	-15.5	3.4	4D
fourth	$Nu_{D,L} = 0.0367\ Ra_{D,L}^{0.411}$	-16.0	1.27	4D
second	$Nu_{D,L} = 0.500\ Ra_{D,L}^{0.231}$	3.44	3.42	5D
third	$Nu_{D,L} = 0.490\ Ra_{D,L}^{0.230}$	0	0	5D
fourth	$Nu_{D,L} = 0.485\ Ra_{D,L}^{0.231}$	0.388	0.372	5D